*Microscopy and Microanalysis* (2021), 1–17
doi:10.1017/S1431927621012782

Microscopy AND Microanalysis

## Original Article

# Impact of Glyphosate-Roundup® in the Ileal Structure of Male and Female Rats: A Morphological and Immunohistochemical Study

Shaimaa M.M. Saleh[1]*, Tasneem A. Elghareeb[2], Mona M. Atia[1] and Mohamed Ahmed Ibrahim Ahmed[2]

[1]Department of Zoology and Entomology, Faculty of Science, Assiut University, Assiut 71516, Egypt and [2]Plant Protection Department, Faculty of Agriculture, Assiut University, Assiut 71526, Egypt

**Abstract**

The current study was aimed to evaluate the effects of variable doses of the weedicide glyphosate on the ileal (the final section of the small intestine) structure of rats of both sexes, using histological, histochemical, and ultrastructural methods. Forty animals were classified into four groups of 10 animals per group (five males and five females). The first group acted as a control, and the remaining groups were treated with glyphosate-Roundup® 25, 50, and 100 mg/kg body weight daily for 15 days. The results indicated extinct histopathological changes manifested in the deformation of villi, foci of leukocytic infiltration in the core of villi, and hyperplasia of goblet cells. Histochemical examination (Alcian blue and Periodic acid–Schiff stain) revealed a strong positive reaction of goblet cells and an increase in their number in all treated groups. In addition, the immunohistochemical investigation revealed the immunoreactivity of matrix metalloproteinase-9 expression. Furthermore, electron microscopic alternations were represented by the deformation of nuclei, destruction of microvilli, and deposition of lipid droplets. Collectively, the present findings indicate that treatment with glyphosate results in extensive morphological alternations to the ileal structure of rats of both sexes and that female rats are more affected than male rats are.

**Key words:** glyphosate, histopathology, ileal structure, immunohistochemistry, morphological alternations

(Received 29 June 2021; revised 20 August 2021; accepted 4 September 2021)

## Introduction

Roundup® is the commercial form of glyphosate (*N*-(phosphonomethyl) glycine), which is a wide-spectrum herbicide. It contains a mixture of glyphosate and other chemical additives that enhance its effect (Bai & Ogbourne, 2016; Mohamed et al., 2016; Zhao et al., 2018). Glyphosate is the world's leading systemic organophosphonate and nonselective herbicide and is used for weed removal (Mesnage et al., 2015). Its commercial formulations are generally in the form of salts that have two main purposes: to increase the effectiveness of the parent compound and to supply a higher solubility of the herbicide (Pérez et al., 2011; Elghareeb et al., 2018). At present, glyphosate is widely applied for agricultural production in most industrial and developing countries (Benbrook, 2016; Saba et al., 2018).

One of the properties of glyphosate is its high solubility in water and its tendency to bind tightly to organic matter and soil within the first 6 inches of soil layers (Duke, 1988). It is generally degraded by soil microbes to amino methylphosphonic acid and $CO_2$. Because of their strong binding properties with soil particles, glyphosate and amino methylphosphonic acid do not move into the groundwater. However, they have the potential to contaminate surface water based on its use patterns and erosion (Ruppel et al., 1977). It has been reported that because glyphosate is used as an agricultural chemical, it has the potential to contaminate harvested food consumed by both humans and cattle (Bai & Ogbourne, 2016; Zhao et al., 2018).

Thus, humans are likely exposed to glyphosate residues from the consumption of vegetables and fruits. In this regard, several studies have found the presence of glyphosate in the urine of the general population (Conrad et al., 2016). This evidence provides a warning sign of the risk involved in using glyphosate to eliminate weeds.

The glyphosate herbicide prevents the synthesis of protein due to the accumulation of shikimate-3-phosphate (Gomes et al., 2014). Plants and some microorganisms have the ability for only shikimate aromatic synthesis (Connolly et al., 2018), but exposure to glyphosate is not fatal to mammals (Mesnage et al., 2015). Many different reasons have been suggested to play an important role in the toxicity in humans and some animals exposed to glyphosate, one of which is the deterioration of the antioxidant defense mechanism (Connolly et al., 2018). This suggestion is based on the report by Turkmen et al. (2019), who reported that exposure to glyphosate produced extensive oxidative stress in tissues. Previously, biological disorders in public health associated with diet were attributed to glyphosate. These disorders include digestive tissue and liver diseases, among others (Samsel & Seneff, 2013).

Matrix metalloproteinases (MMPs) are a large family of zinc- and calcium-containing endopeptidases. There are several classes of MMPs, including stromelysins, gelatinases, matrilysins, and

*Corresponding author: Shaimaa M.M. Saleh, E-mail: shaimaasaleh@aun.edu.eg

**Cite this article: Saleh SMM, Elghareeb TA, Atia MM, Ahmed MAI** (2021) Impact of Glyphosate-Roundup® in the Ileal Structure of Male and Female Rats: A Morphological and Immunohistochemical Study. *Microsc Microanal*. doi:10.1017/S1431927621012782

collagenases (Cathcart et al., 2015). Such a classification is related to their ability to cleave extracellular matrix substrates. Of all types of MMPs, MMP9 is a distinctive type as it contributes to the activation of various signaling molecules and pathways through cancer and inflammation while also being inactive in normal tissues (Vandooren et al., 2013). It is the most one studied MMPs as a mediator of inflammatory bowel disease. MMP9 is commonly secreted by many cells, such as epithelial cells, immune cells, neutrophils, and sometimes by macrophages during inflammation (O'Sullivan et al., 2015).

The ileum is an important organ, which is responsible for absorption of any final nutrients. Thus, morphological and immunohistochemical studies are essential for evaluating the impact of different doses of glyphosate on the ileum structure of rat of both sexes. By doing so, it is expected that the knowledge gained in these studies will contribute to a better understanding of the dangers of using glyphosate for controlling weeds.

## Materials and Methods

### Ethical Approval

Experimental setup and animals handling were approved by the Research, Ethical Committee of the Faculty of Science, Assuit University, Assuit, Egypt. All methods were performed in accordance with the relevant guidelines and regulations.

### Chemicals

Roundup (glyphosate 48% WSC, Monsanto Co.) was obtained from the Central Agricultural Pesticide Laboratory in Dokki, Giza, Egypt.

### Animal and Experimental Design

Forty healthy adult male and virgin female albino rats (12 weeks old, 130 ± 230 g) were maintained under a normal day/night schedule (12 h light:12 h dark) at room temperature (25 ± 2°C). They were supplied with standard laboratory care and fed diet and tap water *ad libitum* throughout the experimental period. The animals were bought from the Assiut University Joint Animal Breeding, Assiut, Egypt.

After 3 weeks of acclimatization, the rats were grouped randomly into four groups of 10 animals each [five males (M) and five females (F)]: rats from group 1 served as the control [control males (CM) and control females (CF)] and received an oral administration of distilled water. Group 2 (M25 and F25) rats were treated with 25 mg/kg body weight (bwt) glyphosate. Group 3 (M50 and F50) rats were treated with 50 mg/kg bwt glyphosate. Group 4 (M100 and F100) rats were treated with 100 mg/kg bwt glyphosate.

All treated groups received an oral administration by gavage of glyphosate herbicide diluted in distilled water on a daily basis for 15 days. This period was chosen based on the work of El-Shenawy (2009). Ileum tissues were collected at the end of this period.

### Tissue Preparation for General Histological, Histochemical, and Immunohistochemical Analysis under a Light Microscope

After 15 days of treatment, the rats were sacrificed under ether anesthesia, the abdomen was dissected, and small pieces of the ileum were removed and fixed in formal alcohol for 24 h and then processed using a standard histological procedure. Sections 4- to 6-$\mu$m thick were cut and stained with hematoxylin and eosin (H&E) according to the procedure of Drury & Wallington (1980). Alcian blue and Periodic acid–Schiff stain (ALB/PAS) were used to demonstrate goblet cell mucin (Kiernan, 2001). Some paraffin sections were used for immunohistochemistry. All sections were examined under light microscopy, and photographs were taken.

To assess MMP9 (a marker for extracellular matrix degradation) in our samples, the immunoperoxidase peroxidase/anti-peroxidase reaction was performed using rabbit anti-human MMP9 monoclonal antibody (clone: EP127; Doc. No. 932-816N-EN; BioGenex kit). Paraffin-embedded tissue specimens were sectioned at a thickness of 4 $\mu$m, deparaffinized in xylene, and then dehydrated in ethanol-graded series solutions. After dewaxing in xylene and rehydrating through graded ethanol, slides were washed in buffer and then incubated in digestive enzymes. Slides were also washed in buffer incubated on slides in UltraVision hydrogen peroxide block for 10 min. After washing in buffer, UltraVision Block was applied for 5 min at room temperature. The primary antibody was then applied at room temperature for 1 h, followed by overnight incubation at 4°C, washing in buffer again, and applying primary antibody enhancer for 10 min at room temperature. Subsequently, HRP polymer was applied for 15 min and incubated with peroxidase-compatible chromogen. Counterstain and coverslip using an aqueous mounting media were finally used.

MMP9 immunohistochemical staining appears as a positive cytoplasmic reaction in the inflammatory, epithelial, and endothelial cells and was visualized as brown granules in the cytoplasm contents.

### Transmission Electron Microscope

Small specimens were taken from the ileum after scarifying and fixed in 5% cold glutaraldehyde for 24 h. The specimens were then washed in cacodylate buffer (pH 7.2) with three to four changes of 20 min for each change and post-fixed in cold osmium tetraoxide for 2 h. Thereafter, the specimens were washed in four changes of cacodylate buffer for 20 min each. The dehydration process was executed using ascending grades of ethyl alcohol of 30, 50, and 70%, each for 2 h, with two changes of 90 and 100% for 30 min each. Embedding was carried out in Epon 812. The embedded samples were kept in an incubator at 35°C for 1 day, at 45°C for another day, and at 60°C for 3 days (Woods & Stirling, 2008). An LKB ultramicrotome (Germany) was used to prepare semithin sections of 0.5–1 $\mu$m, which then were stained with toluidine blue, investigated with a light microscope, and photographed. Ultrathin sections (50–80 nm) from selected areas of the trimmed blocks were taken and collected on a copper grid. The ultrathin sections were contrasted with uranyl acetate for 10 min and with lead citrate for 5 min, examined by transmission electron microscopy (JEOL 100 CX; JEOL, Japan), and photographed at 80 kV in the Assiut University Electron Microscopy Unit.

### Morphometric Analysis

H&E-stained sections were used for an assessment conducted with the computerized image analysis software system, Image J (NIH). Before each analysis, spatial calibration was performed. Five representative pictures were selected from each group. The

following histomorphometric parameters of the ileum section stained with H&E were assessed using a magnification ×10: width of villi (from the half region in micrometers)/7 villi and length of villi (from the tip to base in micrometers)/7 villi. Finally, the number of goblet cells stained by ALB/PAS was expressed as the total number of positive ALB/PAS per 7 villus (×10).

### Statistical Analysis

A close comparison was made between the data obtained from the normal group and those from the treated groups. The outcomes of the comparison were expressed as means ± standard error. One-way analysis of variance was used to test the differences between the means, followed by Student–Newman–Keuls test for multiple comparisons. These analyses were carried out using the computer Prism 5.0 Package (Graph and Software, Inc, San Diego, USA) and Microsoft Excel program. The minimum level of statistical significance was set at $p < 0.05$, 0.01, or 0.001.

## Results

### H&E Stain and Morphometric Analysis of Length and Thickness of the Villi

In the control rats, the ileal mucosa was built up of numerous villi, through which the connective tissue of the lamina propria containing the simple tubular glands as the crypts of Lieberkühn was found (Figs. 1a, 1b). The epithelium lining of the villi was composed of the absorptive columnar epithelial cells (enterocytes), goblet cells, and Paneth cell. The predominant cell type was the enterocytes, which have striated borders, finely granular cytoplasm, and oval, basally located nuclei. The goblet cells were scattered between the enterocytes. The lamina propria of the mucosa was formed of fine connective tissue containing lymphocytes, fibroblasts, and blood capillaries (Fig. 1b).

The histological examination of the M25 treated group revealed marked histopathological alternation. These alternations were characterized by villi that appeared either deformed and irregular or short and atrophied with desquamated epithelium (Fig. 1c). Some enterocytes of the villi were completely lost (Fig. 1d), and leukocytic infiltrations were aggregated, forming foci in the core of the villi (Fig. 1c). The lamina propria in the core of the villi was detached from the basement membrane, with empty spaces remaining. Meanwhile, many dilated lacteal in the lamina propria were observed. However, other villi were completely depleted from the lamina propria (Fig. 1d). In the F25 treated group, the villi appeared completely atrophied, leaving a portion of the remnant goblet cells. However, other villi appeared destructed, and a small remnant of damaged villi debris was observed in the lumen (Fig. 2a). In addition, there were broad and blunt deformed villi with disruption and sloughing of the surface epithelium. Moreover, the contents of the lamina propria were degenerated. The enterocytes of some crypts showed necrosis (Fig. 2b).

The histological examination of the M50 treated group revealed an increase in the thickness of many deformed villi with degeneration of their lamina propria, leaving many empty spaces, and their epithelial surface showed necrosis (Figs. 2c, 2d). Massive detachment of the lamina propria from the basement membrane, darkly stained cytoplasm, and nuclei of the epithelium lining of the crypts, and damage of the basement membrane were observed (Fig. 2d). The histopathological changes in the F50 treated group appeared more excessive than those of the M50 treated group. These changes were in the form of excessive destruction of villi, and the lumen was filled with much debris (Fig. 3a). Hyperplasia of goblet cells was also prominent (Fig. 3b).

Microscopic investigation of the M100 and F100 treated groups showed pathological changes similar to those of the previous treated (M50 and F50), but some other changes appeared more extensive. In the M100 treated group, the extensive changes represented by most of the villi were more atrophied. They were split from the submucosa and showed hyperchromatic epithelial cells. In addition, a large gap in the core area of the villi was prominent. Moreover, the crypts conjugated without any contact with the villi (Fig. 3c). In many large areas, the villi appeared more widened and depleted from the lamina propria (Fig. 3d). On the other hand, the pathological changes in the F100 treated group appeared similar to those of the M100 treated group, but some other pathological changes differed from the latter group. The differences were the ileal tissue loss of their architecture, shortness of the villi, complete destruction of most of the lower part of villi (Figs. 4a, 4b), and noticeably large spaces in between disrupted short villi (Fig. 4c).

### Morphometric Analysis of H&E Sections

Statistical analysis of the length of the villi revealed significant differences in the treated groups as compared with the control group. The treated groups exhibited a shorter length than that in the control group. The villi of the M50 group appeared to be shorter than those of the M25 group, with significant differences ($p < 0.005$). However, the other treated groups showed no significant between-group differences in their villi length (Fig. 4d).

Morphometric analysis of the thickness of the villi showed a significant increase in all treated groups as compared with the control group, with statistical differences. The M50 group had a greater increase in villi thickness than the other treated groups did, with highly significant differences. There were no statistically significant differences in thickness among the treated groups (Fig. 4e).

### ALB/PAS Stain and Morphometric Analysis of Goblet Cell Counts

A close examination of the ALB/PAS reaction of the control ileum revealed a strong positive reaction in the goblet cells of the villi and crypts and the brush border of enterocytes (Fig. 5a). In the M25 treated group, there was a strong positive reaction of goblet cells of villi, crypts, and brush borders. However, a negative reaction in some places of damaged brush borders was also observed (Fig. 5b). In the F25 treated group, there was an increase in the number of goblet cells in some intact villi compared with the control group, with a prominent, strong positivity in the goblet cells (Fig. 5c). Morphometric analysis of the mean account of goblet cells showed a significant difference ($p < 0.001$) between the control group and the M25 and F25 groups and also between the M25 and F25 treated groups ($p < 0.001$; Fig. 5h).

The positivity of the goblet cells in the M50 treated group was strong, and the number of goblet cells decreased as compared with previous treated groups (Fig. 5d). Statistically, there was no significant difference in the number of goblet cells between the M50 and M25 treated groups, but a significant difference

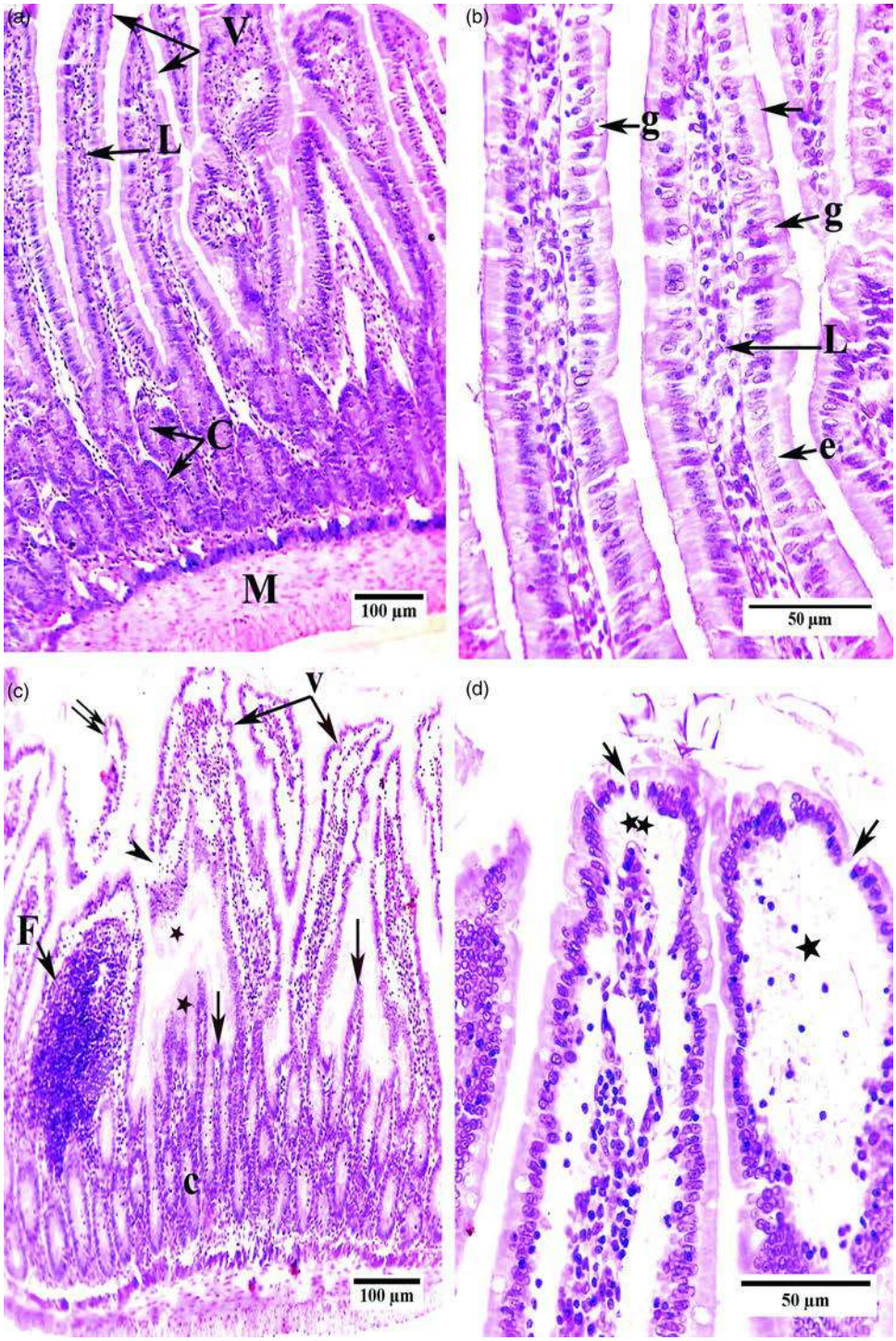


Fig. 1 - Colour online, Colour in print

**Fig. 1.** H&E stain of ileum structure showing (**a,b**) control group: (**a**) normal structure of villi (V), lamina propria (L), crypts of Lieberkühn (C), and muscular layer (M); (**b**) well-developed villi with normal enterocyte (e), covered by brush border (arrow), goblet cells (g), and lamina propria (L). (**c,d**) M25 treated group: (c) the villi appeared with many structural changes; deformed and irregularity in shape (v), short atrophied (arrow), disrupted with desquamation of their epithelium covering (star), destruction of villi (arrowhead), and some debris of destructed villi in the lumen (arrows). Crypts of Lieberkühn (c) and foci of leukocytic infiltration in the lamina propria of villus (F). (**d**) Lamina propria lifting from the surface epithelium leaving empty space (two stars), and villus depleted completely from lamina propria (star) and destruction of some enterocytes (arrow).

($p < 0.001$) was found in the comparison with the F25 treated group (Fig. 5h). In the F50 treated group, a strong positive reaction in the goblet cells and an increase in their number were observed (Fig. 5e). Meanwhile, there was a negative reaction in many goblet cells. There was a significant difference ($p < 0.001$) between the F50 and M50 treated groups and also between the F50 and control group, but no differences were observed between the F50 and F25 treated groups (Fig. 5h).

The last groups, M100 and F100, showed a strong positive result of ALB/PAS in the cells with hyperplasia of

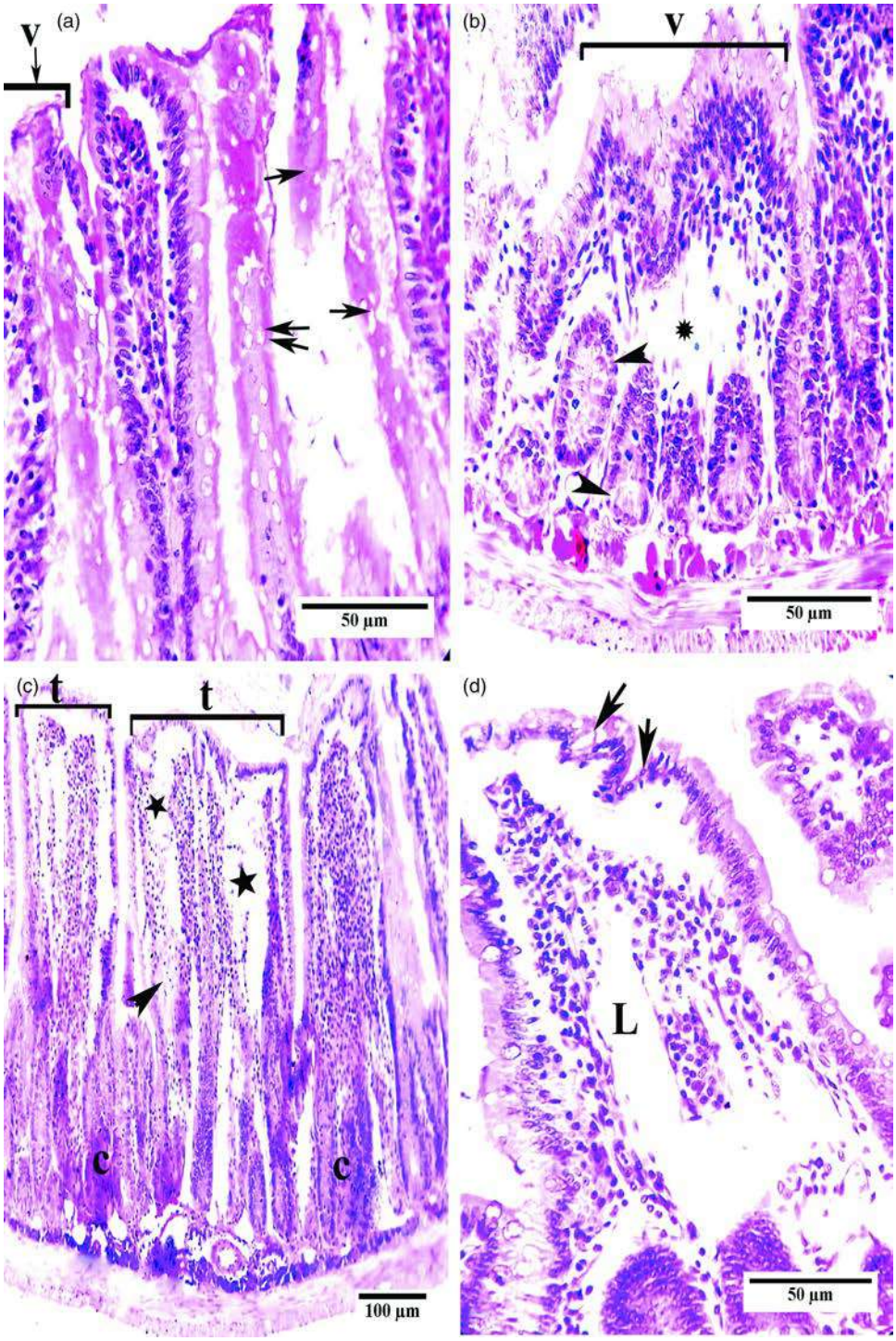


Fig. 2 - Colour online, Colour in print

**Fig. 2.** H&E stain of ileum structure showing (**a,b**) F25 treated group: (**a**) hyperplasia of goblet cells (arrows) and necrosis of most epithelial covering (arrow). The villi appeared complete destructed (v) and degenerated leaving much debris in the lumen (arrow). (**b**) Broad and blunt deformed villi (v) with disruption and sloughing of their surface epithelium, decomposition of most lamina propria content (* ), and degenerated of many endocytic cells of crypts (arrowheads). (**c,d**) M50 treated group ileum showing widening of many villi (t) with degeneration of their lamina propria leaving many empty spaces (stars) and necrosis of their epithelial surface (arrow). Necrotic area (arrowhead), darkly stained cytoplasm, and the nuclei of the epithelium lining of the crypts (c) and many degenerated areas of lamina propria (L).

goblet cells and also in some sloughing epithelial cells (Figs. 5f, 5g). Statistically, the number of goblet cells was significantly decreased in the M100 treated group ( $p < 0.001$) as compared with M25 and M50 treated groups. Meanwhile, the decrease in the number of goblet cells in the F100 treated group was also significantly prominent as compared with that of the F25 and F50 treated groups ( $p < 0.001$; Fig. 5h). It is worth mentioning that the number of goblet cells increased in the groups of treatment females as compared with the treated and control male groups.

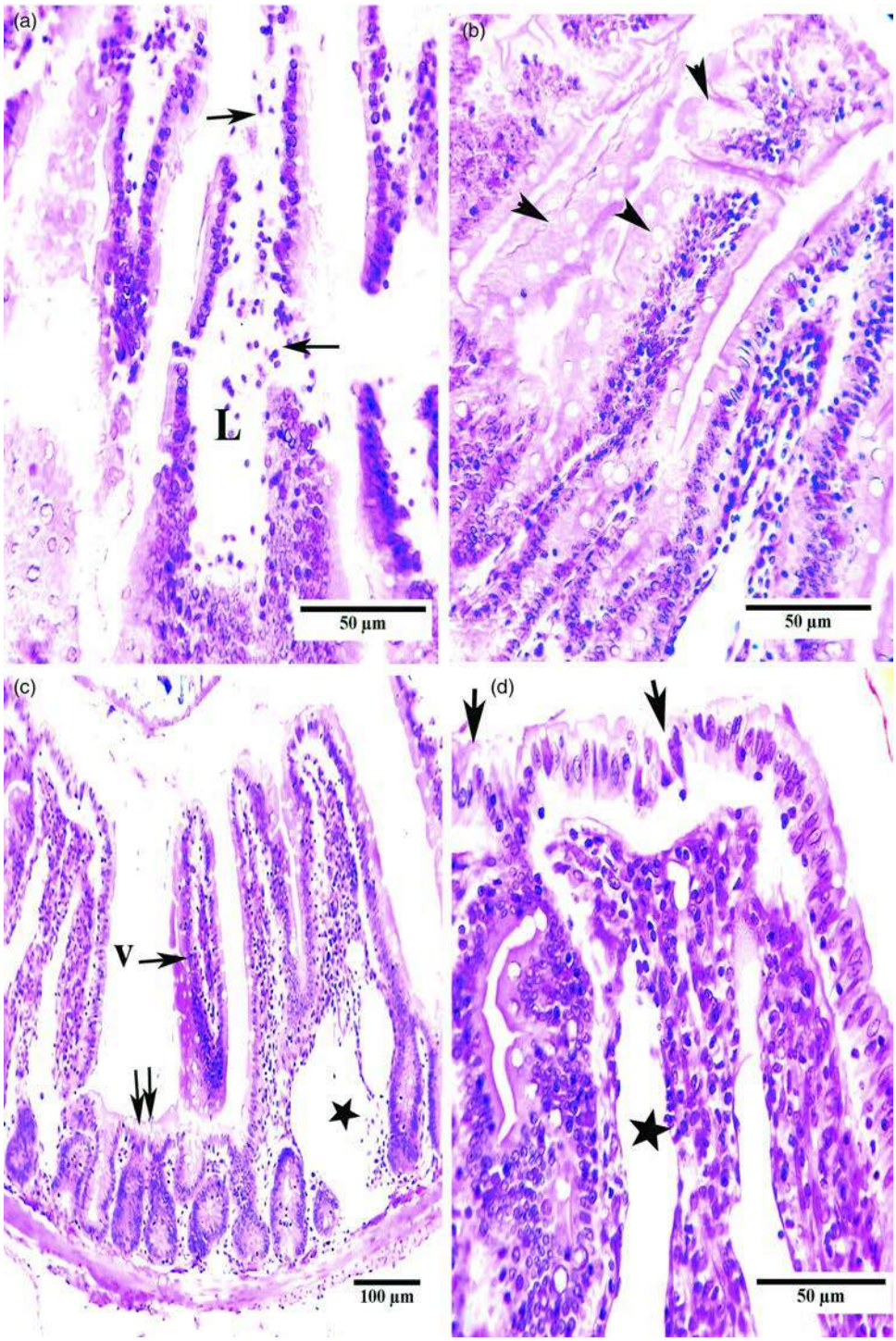


Fig. 3 - Colour online, Colour in print

**Fig. 3.** H&E stain of ileum structure showing (**a,b**) F50 treated group: (**a**) destruction of most epithelial covering (arrow) and lamina propria (L) of many villi. (**b**) Much hyperplasia of villi goblet cells (arrowheads). (**c,d**) M100 treated group: (**c**) atrophied villi (v) split from submucosa with hyperchromatic epithelial cells and hyperplasia of their goblet cells. A large gap area (star) and conjugated crypts (arrows) with no contact with any villi were observed. Note: space devoid from villi. (**d**) Broad villi, loss of parts of the lining mucosa cells (↑) and dilatation in lamina propria (star).

### *Immunohistochemistry for MMP9 Expression*

The immunohistochemical stain for MMP9 of the control group revealed a negative cytoplasmic reaction of the mucosal lamina propria of the villi and mucosal epithelial cells (Fig. 6a). In the M25 treated group, a strong positive immunoreaction occurred in the cytoplasm of inflammatory cells within the lamina propria of villi (Fig. 6b). Such a positive reaction was also observed in the F25 treated group (Fig. 6c).

The immunohistochemistry in the ileal sections for MMP9 of the M50 treated group also showed a strong positive reactivity around the edges of the dilated area in lamina propria of villi and degenerated mucosal cells (Fig. 6d). Meanwhile, the same positive reaction was observed in the F50 treated group (Fig. 7a).

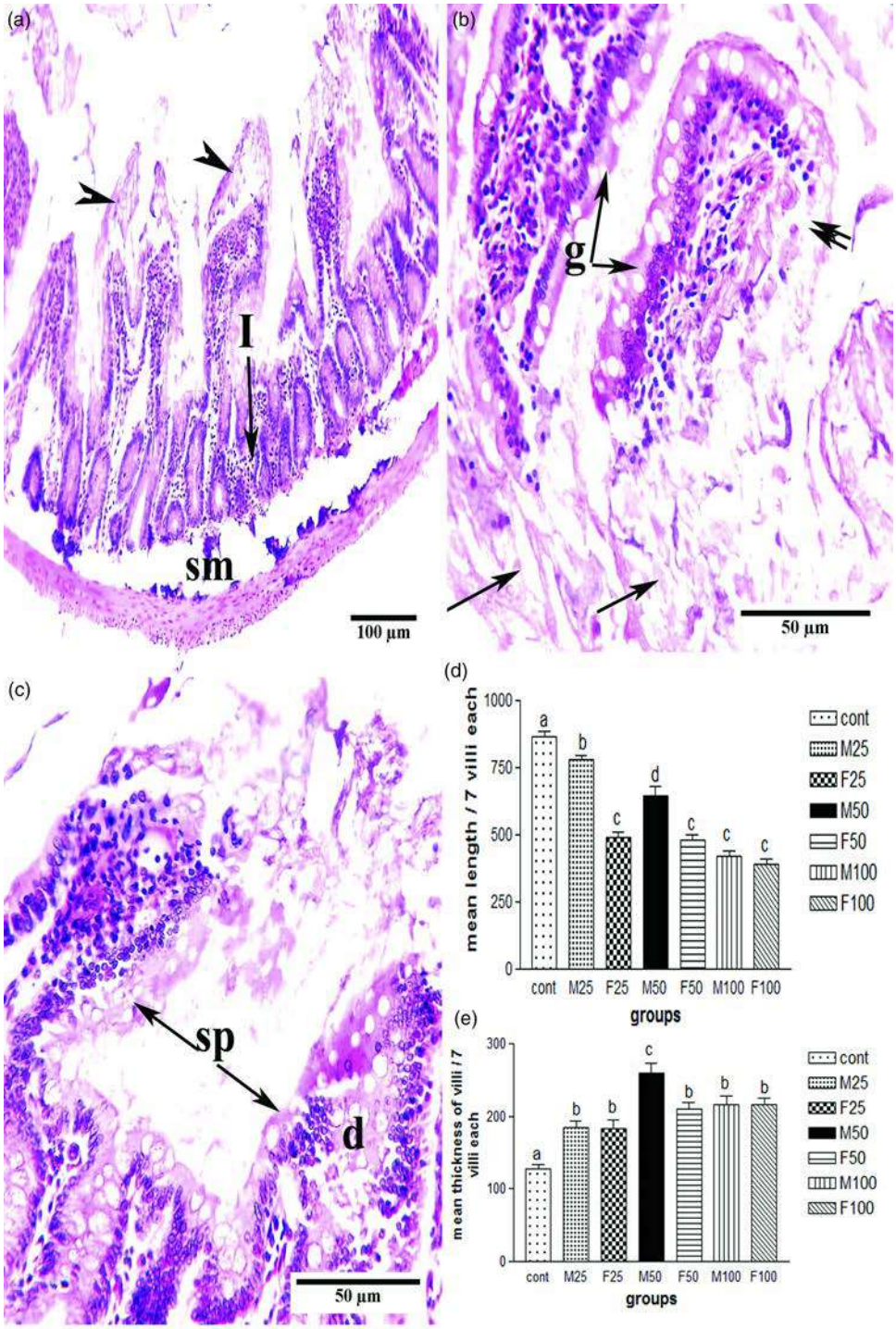


Fig. 4 - Colour online, Colour in print

**Fig. 4.** H&E stain of ileum showing (**a–c**) F100 treated group: (**a**) atrophied most of villi and appeared very short with extensive sloughing of their surface epithelium (arrowhead), inflammatory cells in between crypts (I) and disruption of submucosa layer (sm). (**b**) Complete destruction of lower part of villi leaving many debris in the lumen (arrow), increase in the number of goblet cells (g), and disintegration of epithelial covering (arrows). (**c**) Large space (sp) in between disrupted villi (d). (**d,e**) Mean values of morphometric analysis of ileum (**d**), length of villi, and (**e**) thickness of villi in control and different treated groups of male and female rats.

In the M100 treated group, the MMP9 positive reaction increased in many of the epithelial linings of dilated blood vessels and lamina propria cells and also showed a mild reaction in a few mucosal cells of the villi (Fig. 7b). Such a positive MMP9 immunoreactivity was also prominent in the F100 treated group. However, the F100 treated group showed different positive reaction places more than the M100 group do. The immunoreactivity also appeared in a large degenerated area under mucosal cells (Fig. 7c).

### *Electron Microscopy Study*

Semithin sections of control male and female rats appeared similar to each other. Normal villi with columnar epithelial lined with

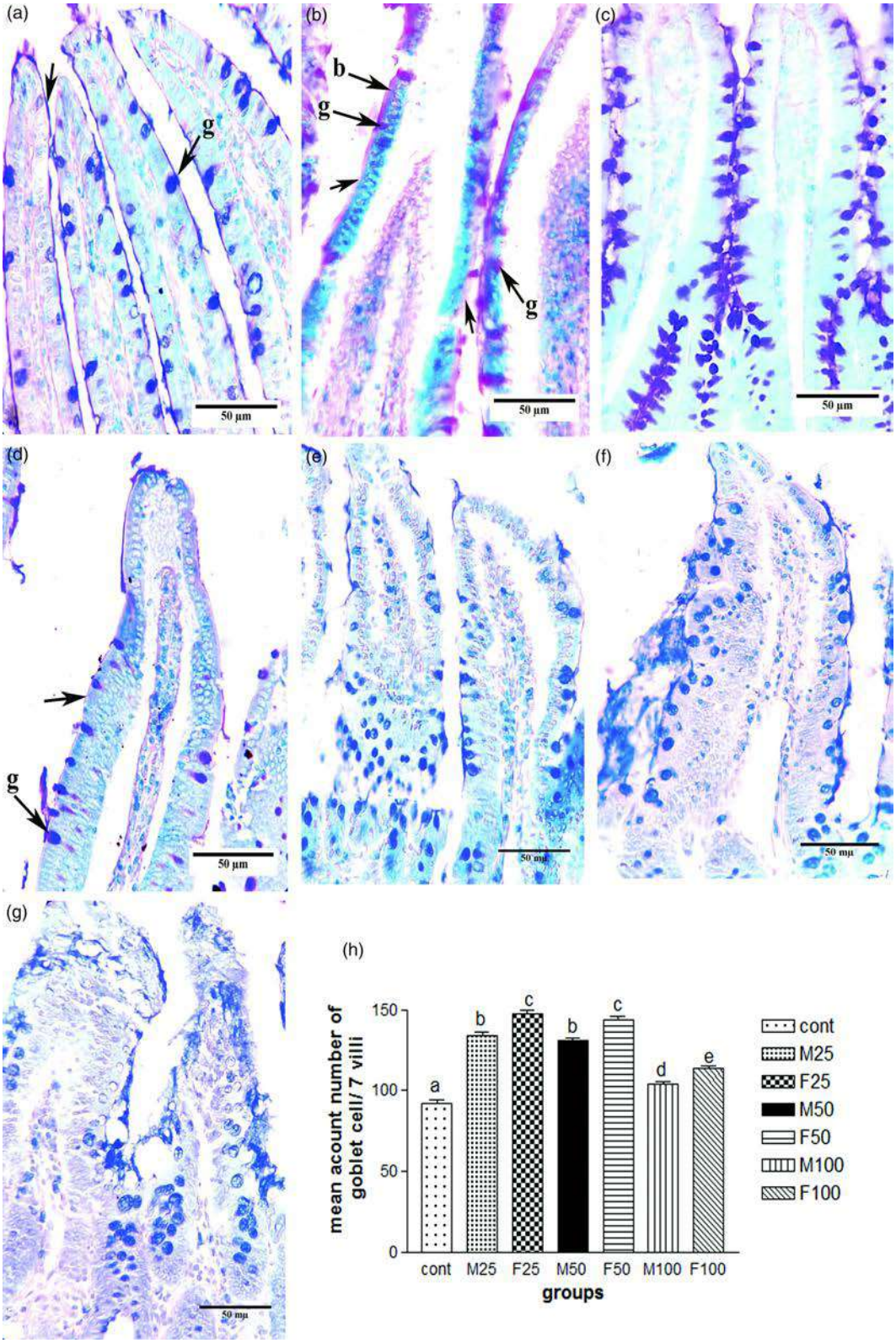


Fig. 5 - Colour online, Colour in print

**Fig. 5.** ALB/PAS stain of ileum showing (**a**) control group: strong positive in goblet cells of villi (g) and brush border (arrow). (**b**) M25 treated group: positive reaction in goblet cells of villi (g), brush border (b). Note: negative reaction in damaged brush border places (arrow). (**c**) F25 treated group: increase number of goblet cells in intact villi. (**d**) M50 treated group: strong positive reaction in goblet cells of villi (g) and a negative reaction in damaged brush border places (arrow). (**e**) F50 treated group: strong positive reaction in goblet cells hyperplasia. (**f**) M100 treated group: strong positive reaction in goblet cells. (**g**) F100 treated group: high strong positive reaction of goblet cells and their hyperplasia. (**h**) Mean values of morphometric analysis of goblet cell account number in control and different treated groups of male and female rats.

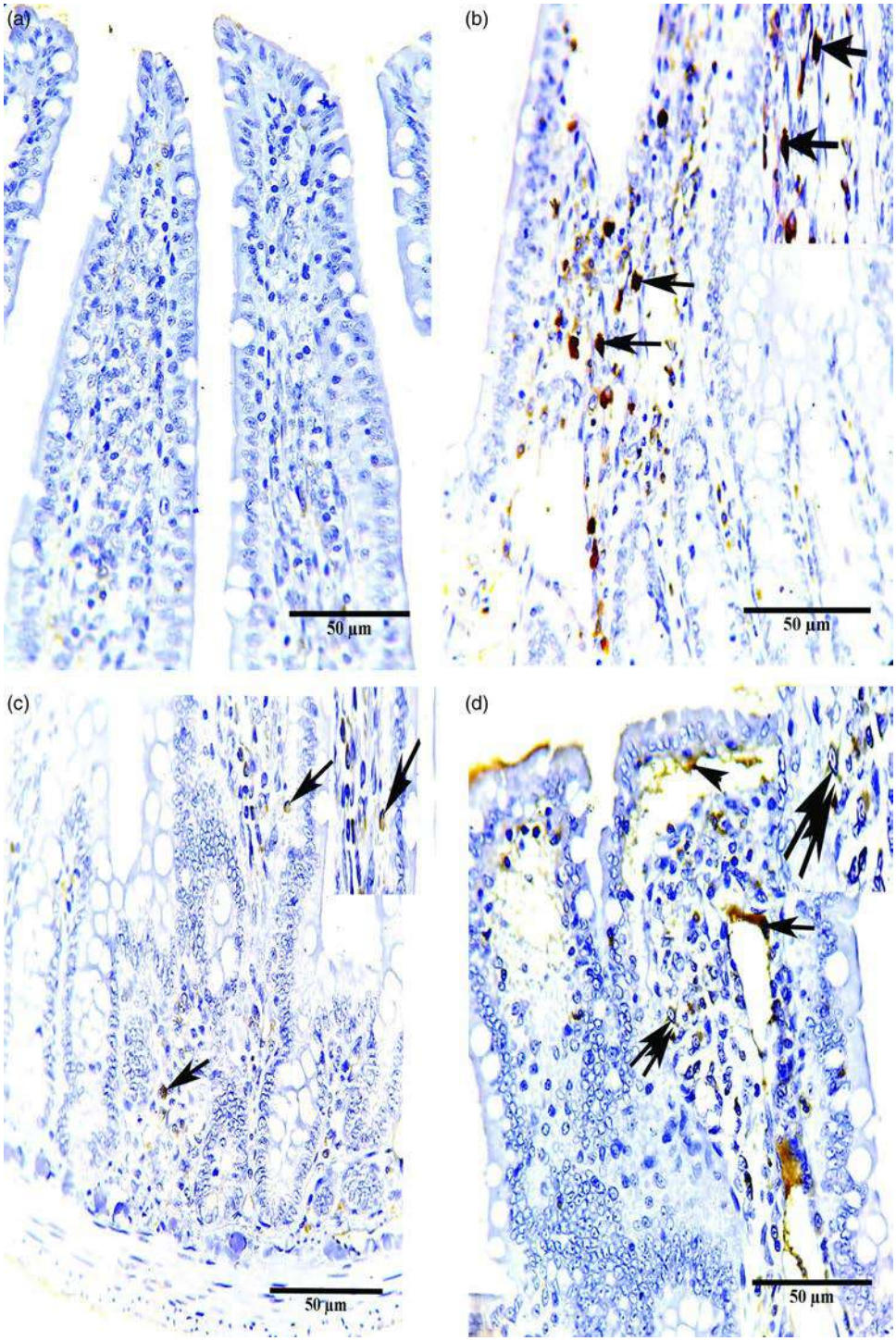


Fig. 6 - Colour online, Colour in print

**Fig. 6.** Immunohistochemistry in the ileal sections for MMP9 showing control group: (**a**) –ve immunoreaction in cells of the lamina propria and mucosal cells. (**b**) M25 treated group: abundant of strong +ve cytoplasmic immunoreaction (arrows) in the inflammatory cells of lamina propria of villi. (**c**) F25 treated group: +ve MMP9 activity on the cytoplasmic of the inflammatory cells of lamina propria (↑). (**d**) M50 treated group: strong positive immunoreactivity in inflammatory cells within lamina propria of villi (↑↑), around dilated area in lamina propria of villi (↑), and degenerated mucosal cells (arrowhead).

a brush border, goblet cells, and normal compact lamina propria were present (Fig. 8a).

Electron microscopy examinations of the ileal mucosa of the control group revealed that the ileal mucosal epithelium was composed of one layer that contained many types of cells resting on a basement membrane. The absorptive columnar cells had ovoid basally located nuclei. Each nucleus had a prominent nucleolus and heterochromatin clumps, mostly adjacent to the inner surface of the nuclear envelope. The cells were provided with microvilli at their luminal surfaces. The microvilli appear as closely packed, long, parallel projections on the apical surfaces of the epithelial cells (Figs. 8b, 8c).

In the M25 treated group, the enterocytes of the villi revealed vacuolation of their cytoplasm and damage of their basement

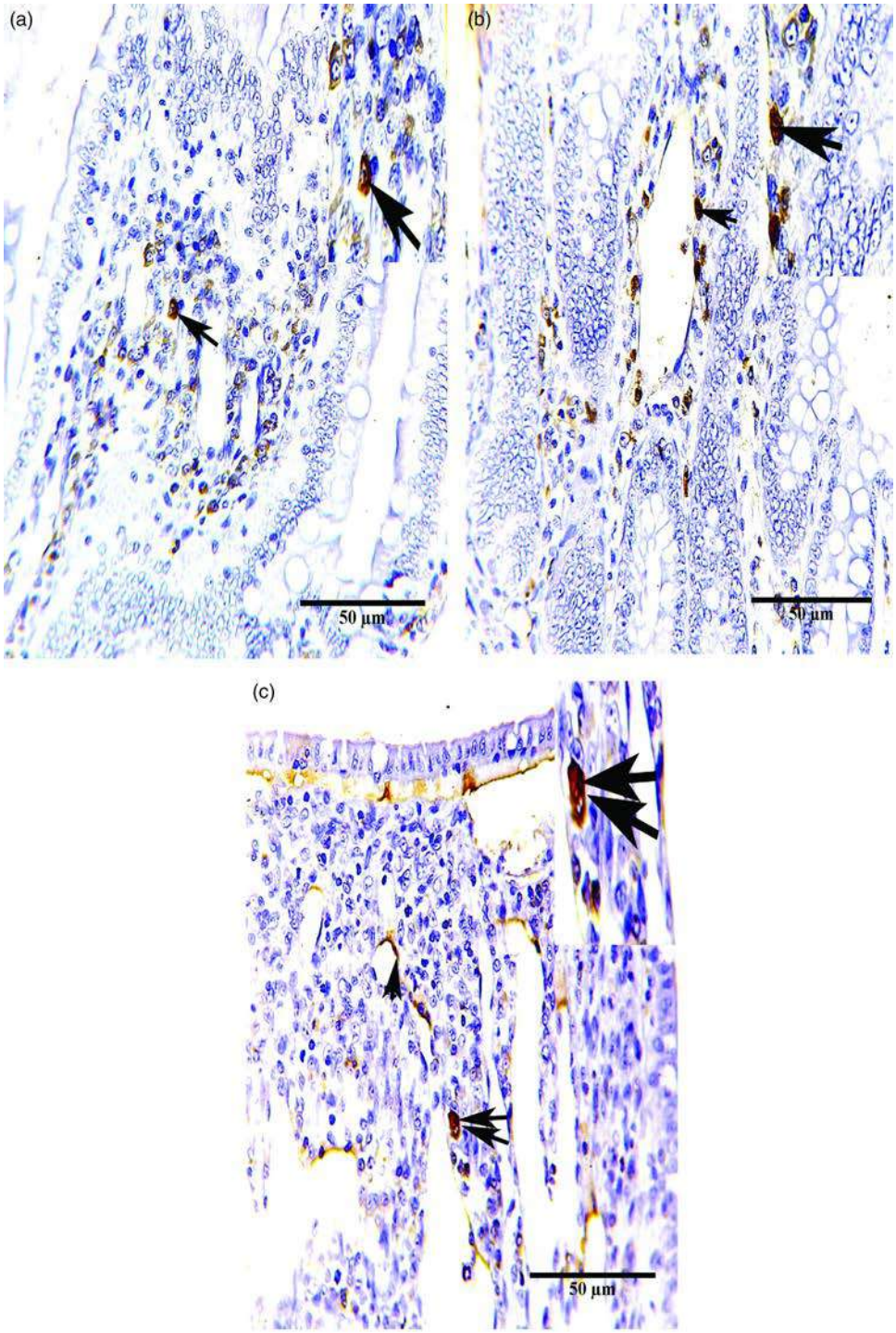


Fig. 7 - Colour online, Colour in print

**Fig. 7.** Immunohistochemistry in the ileal sections for MMP9 showing (**a**) F50 treated group: positive immunoreaction in inflammatory cells within lamina propria of villi (↑). (**b**) M100 treated group: +ve immunoreactivity in the lining epithelium of dilated blood vessel (arrowheads), lamina propria cells (↑), and mild reaction in mucosal cells of villi (arrowhead). (**c**) F100 treated group: immunoreactivity in cytoplasmic of lining epithelium of blood vessel (arrowhead) and lamina propria cells (↑↑).

membrane, and many of the nuclei showed pyknosis. Large congestion of dilated blood vessel in the lamina propria was also noted (Fig. 8d).

The ultrastructural examination of the M25 treated group revealed degeneration of many enterocytes with abundant lipid droplets. The nuclei appeared with pyknosis, and the nuclear membrane of the other nuclei showed irregularity and peripheral heterochromatin migration (Fig. 8e). Moreover, rarified cytoplasm and disrupted microvilli were obvious (Figs. 8e, 8f). However, in the F25 treated group, the disorganization of the cell, many rarified cytoplasm areas, and disintegration of the endoplasmic reticulum cristae were also observed (Fig. 9a).

The ultrastructural examination of the ileum in the M50 treated group revealed many enterocytes with degenerated cytoplasm. Irregularly peaked nuclei and invagination of the nuclear membrane of other nuclei were also evident (Fig. 9b).

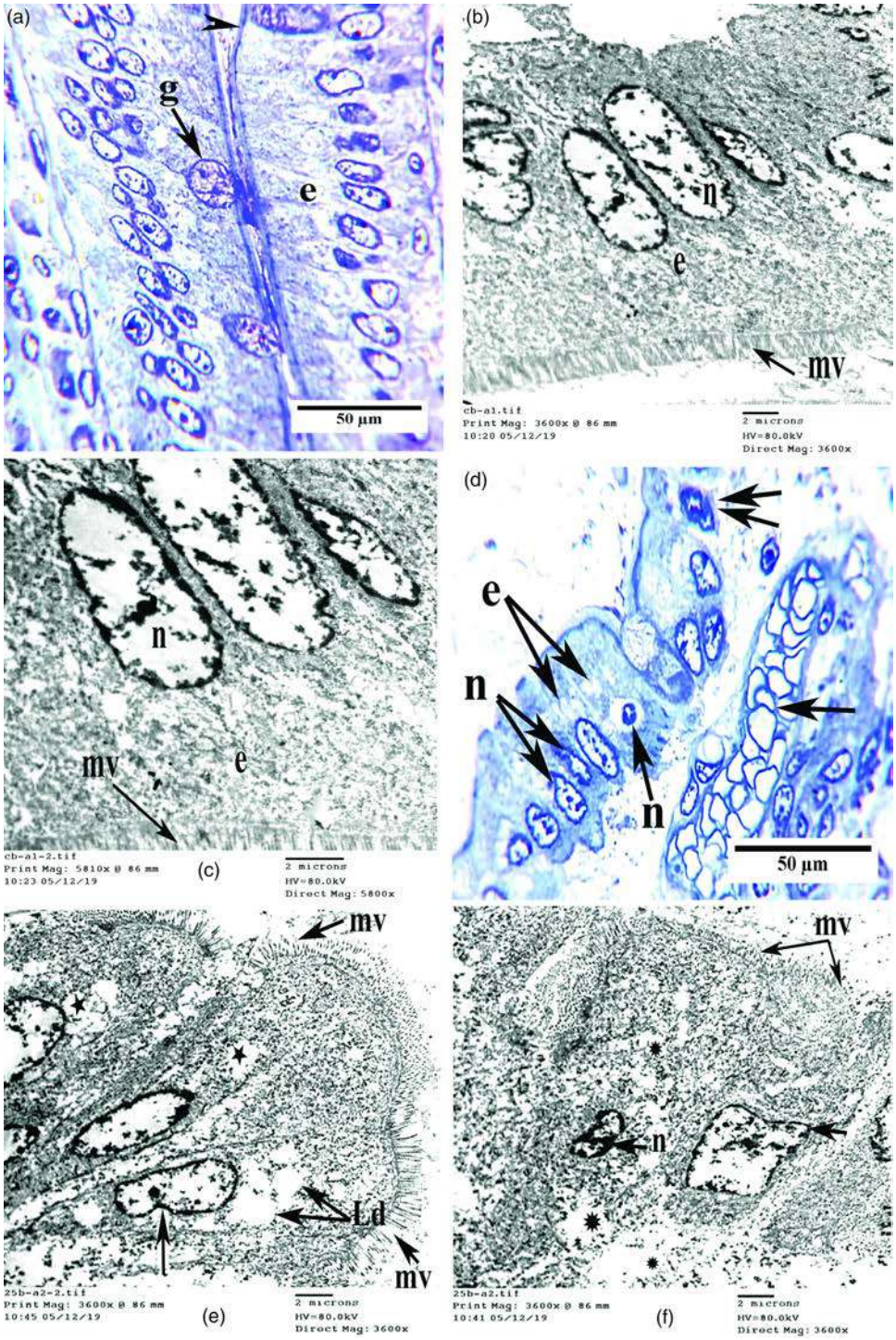


Fig. 8 - Colour online, Colour in print

**Fig. 8.** (**a–c**) Control group: (**a**) semithin section showing normal architecture of villi with columnar epithelial (enterocytes) (e), lined with brush border (arrowhead), and goblet cells (g). (**b,c**) Electron micrograph of villus segment cell showing columnar cells (enterocyte) (e), with prominent oval nuclei (n), and covered completely with regular microvilli (mv). (**d**) M25 treated group: semithin section showing congested blood vessel in lamina propria (↑), enterocytes with vaculated cytoplasm (e), and with damaged basement membrane (↑↑) and pyknosis of many of nuclei (n). (**e,f**) M25 treated group: electron microscopy of villus segment cell showing (**e**) degeneration of many enterocytes with lipid droplets (Ld) and also rarified cytoplasm (*) and disrupted microvilli (mv). (**f**) The nuclei appeared pyknotic (n) and the nuclear membrane of the nuclei appeared irregular and peripheral heterochromatin migration (↑).

The examination of the semithin sections of the F50 treated group showed some changes that were similar to those of the M50 treated group, but other changes appeared more frequently than in a previously treated group (M25 treated group). These changes were manifested in the presence of a strange structure between the lamina propria and epithelial covering, which may be like an edema and pyknosis of the nuclei of many enterocytes as compared with the previously treated groups (Fig. 9c). Although the electron microscopic investigation of that group showed aggregation of cytoplasmic organelles around the nuclei, there were large areas of rarified cytoplasm and shrunken nuclei (Fig. 9d).

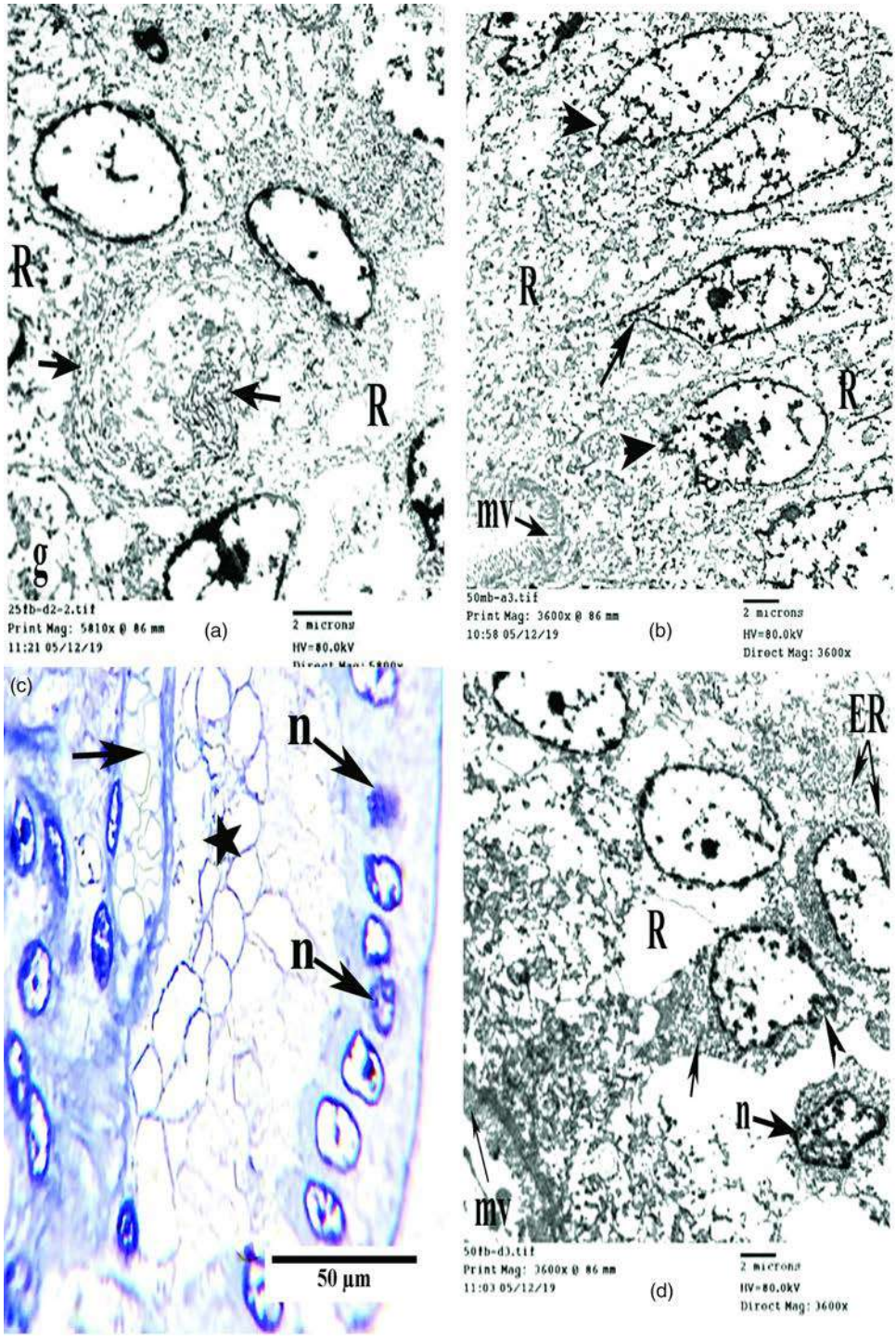


Fig. 9 - Colour online, Colour in print

**Fig. 9.** (**a**) F25 treated group: electron microscopy of villus segment cell showing disorganization of the cells with many rarified cytoplasm areas (R). Disintegration of the ER cristae (↑) was also observed. Note: goblet cell (g). (**b**) M50 treated group: electron micrograph of villus segment cell showing enterocytes with many rarified cytoplasm (R) and irregular peaked nuclei (↑), invagination of nuclear membrane of other nuclear cell (arrowhead) and microvilli (mv). (**c,d**). F50 treated group: (**c**) semithin section showing congested blood vessel (↑), strange structure may be edema between lamina propria and epithelial covering (star), and many pyknotic nuclei were observed (n); and (**d**) electron microscopy of villus segment cell showing aggregation of cytoplasm organelles around nuclei (↑), large areas of rarified cytoplasm (R), shrinked nucleus (n), destructed endoplasmic reticulum (ER), and microvilli (mv).

The examination of the semithin sections and electron microscopy of the M100 treated group revealed that the nuclei appeared deeply indented and irregular with peripheral condensed chromatin (Fig. 10b) and others with pyknotic nuclei (Fig. 10a). In addition, the distraction of the microvilli was prominent (Fig. 10b). Meanwhile, the F100 treated group demonstrated deterioration of the nuclei, which were denoted by a dense, shrunken crescentic nucleus; pyknotic nuclei; irregularity in their shapes (Figs. 10c, 10d); and nuclei with a deflated inside (Fig. 10e).

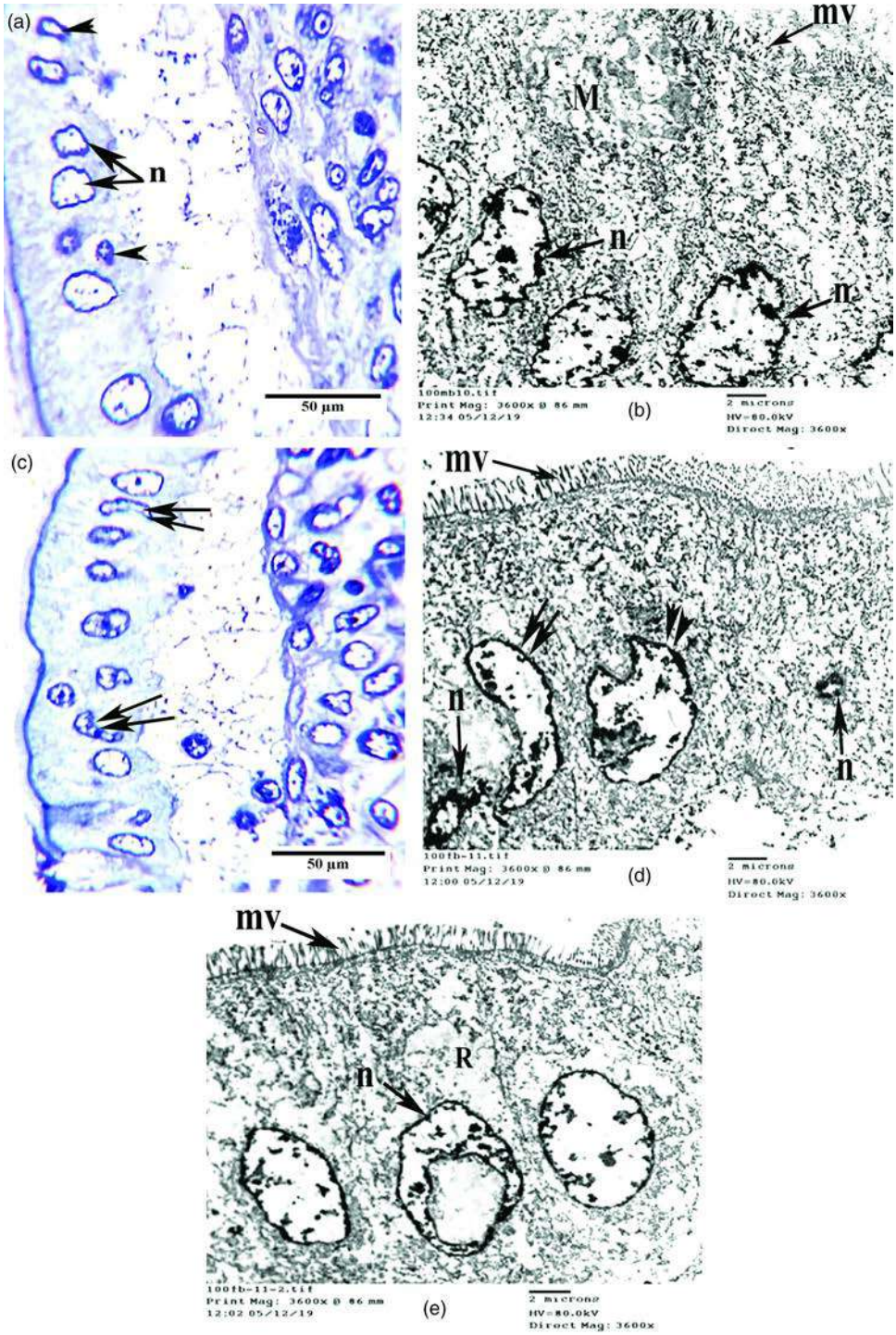


Fig. 10 - Colour online, Colour in print

**Fig. 10.** (**a,b**) M100 treated group: deeply indentation of the nucleus (n) with peripheral condensed chromatin, pyknotic nuclei (arrowhead), mucous secretion of goblet cell (M), and distracted microvilli (mv). (**c–e**) F100 treated group showing (**c,d**) deterioration of the nuclei; dense shrinked crescentic nucleus (↑↑), pyknotic nuclei (n), irregularity in shape (arrowheads), and microvilli (mv). (**e**) The nuclei deflated inside (n) and highly vacuolated cytoplasm (R). Note: (**a,c**) Toluidine blue-stained sections and (**b,d,e**) electron micrograph.

The above results are summarized in Table 1 in terms of the histopathological changes noted in the ileum structure of male and female rats that were administered different doses of glyphosate for 15 days. The change was marked as none (control), (+) mild, (++) moderate, and (+++) severe. Again, the table shows that, in most cases, the responses of the female rats were more than those of the male rats. In addition, the table shows that as the dose of glyphosate increases, the severity of the responses increases.

## Discussion

On the basis of the results in the present investigation, it is evident that exposure to glyphosate has led to distinctive histopathological

**Table 1.** Summary of a Dose-Related Scoring System, According to Histological and Morphometric Analysis.

| | Groups | | | | | | |
|---|---|---|---|---|---|---|---|
| | Control | 25 mg/kg bwt | | 50 mg/kg bwt | | 100 mg/kg bwt | |
| Morphological and Immunohistochemical Changes | Male and Female | Male | Female | Male | Female | Male | Female |
| Shortness of villi | – | + | ++ | ++ | ++ | +++ | +++ |
| Deformation of villi | – | + | +++ | ++ | +++ | ++ | +++ |
| Thickness of villi | – | + | + | +++ | ++ | ++ | ++ |
| Necrosis of villi epithelia | – | + | +++ | ++ | +++ | ++ | +++ |
| Foci of leukocytic infiltration | – | + | – | – | – | – | – |
| Degeneration of lamina propria | – | ++ | +++ | ++ | +++ | ++ | +++ |
| Increase in number of goblet cells | – | ++ | +++ | ++ | +++ | ++ | +++ |
| Nuclear deformation | – | + | ++ | ++ | ++ | +++ | +++ |
| MMP9 expressions | – | ++ | + | ++ | ++ | ++ | +++ |

(–) none, (+) mild, (++) moderate, and (+++) severe.

and subcellular alterations in ileum tissue. It seems that the most extensive changes occurred with the high dose of glyphosate (100 mg/kg bwt) used in the present study.

The most conspicuous alternations after glyphosate exposure were the damage of villi, destruction of enterocytes, deformation in the nucleus, rarified cytoplasm, and detachment of the lamina propria from their lining epithelium. In addition, aggregation of leukocytic infiltration in the core of the villi and hyperplasia of goblet cells with excessive mucus secretion were observed. Moreover, the formation of lipid droplets and blood vessel congestion were noted.

In the present investigation, the alternations in villi were characterized by many changes. Some villi appeared with short atrophy, whereas others showed degeneration and were blunt. These characteristics are in agreement with those reported by Fathi et al. (2020), who observed that the size and height of the villus were lower among different parts of the small intestine of chicken embryo treated with glyphosate. In teleost fish *Channa punctatus*, the toxic effect of Elsan organophosphate pesticide resulted in disruption of the villi structure (Kosik-Bogacka & Kolasa, 2012). Hamdamin et al. (2017) reported that the shortening of villi may be attributed to the formation of duodenitis by glyphosate toxicity. The villi blunting ends have also served as evidence of an important characteristic of mucositis in the intestine, as a side effect of chemotherapy (Tooley et al., 2009). Duncan & Grant (2003) stated that after chemotherapy treatment, the stem cells were damaged, and a short time afterward were divided or differentiated into a specific cell lineage. Because of this process, the regenerated cells were affected, and the villus mucosa was not substituted, which caused a quick loss of structure and function. This observation explains that these signs of mucosal damage may be due to the exposure to any toxic substance such as glyphosate.

Torretta et al. (2018) suggested that in cases of intestinal disease, the damage in the villus is most likely the result of the insufficiency of the villus to absorb many fundamental nutrients, including vitamins B12 and B6, in addition to folate, calcium, and vitamins D and K. In addition, Hershko & Patz (2008) showed that the disturbance in the epithelial lining of the small intestine was related to glyphosate, because of its relation to the breakdown of complex proteins. The present pathological findings are in harmony with the findings of Olaleye et al. (2007) and Samanta et al. (2016*b*), who reported that the alternations in the small intestine were related to the change in oxidative metabolism. Therefore, these histological changes noted in the villus might be viewed as the first warning signs arising from glyphosate exposure.

It is noteworthy that normal goblet cell function has vital implications for the integrity of both the intestinal barrier and innate immunity. The goblet cells secreted mucin in the form of a layer of gel covering the mucosal surface. This layer has two important functions: it prevents large particles from directly contacting the epithelium, and it reduces the rate of diffusion of ions and small solutes across the epithelium. In addition, it provides resistance to pathogen colonization by allowing adhesion of commensal bacteria and exclusion of pathogenic bacteria (Collado et al., 2007).

In this study, the goblet cells indicated hyperplasia and an increase in the amount of mucin. These observations are in line with those of Samanta et al. (2016*a*), who reported a large amount of mucin secretions covering the epithelial cells in fish treated with glyphosate. Senapati et al. (2009) confirmed the presence of a similar pathological lesion in the alimentary tract of *C. punctatus* after exposure to glyphosate. In their investigation, Ramírez-Duarte et al. (2008) reported moderate hyperplasia in the mucus cells of *Piaractus brachypomus* after administration of Roundup. Olubuyide et al. (1984) concluded that the increase in the numbers of goblet cells could be viewed as an adaptive response of the intestine to any external stress. Samanta et al. (2016*a*) noted that the gastric epithelium showed additional secretion of mucus. They used that finding to imply that exposure to glyphosate triggered the activity of the gastric cells and eventually minimized the defense ability of the gastric epithelium from chemical injury and cell lysis. The massive and rapid secretion of mucus of the goblet cell assists in the rejection of pathological changes and also maintains the solidity of the mucus protective layers (Hasnain et al., 2010).

In the present study, leukocytic infiltration was observed in the core of the villi and between crypts, a finding that agrees with the observations of a previous study in the liver of rats exposed to glyphosate (Saleh et al., 2018). Walter & Isreal (1974) suggested that such leukocytic infiltration might be due to the presence of

necrotic cells, which act as disturbing substances that catch the inflammatory cells.

In this work, investigation via electron microscopy revealed many changes. The most conspicuous changes were the rarified cytoplasm, disintegration of rough endoplasmic reticulum (RER) crista, fatty deposition, and deformation of nuclei. Samanta et al. (2016*a*) reported that in *Anabas testudineus,* the epithelium of the stomach and intestine showed damage in the RER as well as a deformed nucleus after exposure to glyphosate. Similar results were reported by Samanta et al. (2016*b*), who found deformation in the RER and fatty deposition in the stomach of freshwater teleostean fish (*Heteropneustes fossilis*) after glyphosate treatment.

Samanta et al. (2016*b*) and Saleh et al. (2018) observed the deposition of lipid droplets in fish and rats exposed to glyphosate, respectively. These observations are in agreement with the present results on the villi epithelium. In Cheville (1988), the presence of an abundant amount of lipid droplets suggested dysfunction in the protein synthesis in the cytoplasm (serving as lipid-metabolizing enzymes and playing an important role in the transport of triglycerides), resulting in blockage of the use of lipid–protein conjugation, and so forth. According to this case, lipids are produced continuously at a normal rate, which causes a gradual accumulation of lipid globules (Holm et al., 1993).

The immunohistochemical examination of MMP9 in the present study showed a cytoplasmic positive reaction of the inflammatory, epithelial, and endothelial cells in treated groups versus the control group. Accordingly, the increase in MMP9 might lead to ulceration and inflammation because of the disintegration of the extracellular components (Lazăr et al., 2015). Ma et al. (2004) indicated that increasing MMP9 might cause dissolution of the cytoplasmic proteins, leading to the disruption of the tight junctions between the epithelial cells. Impairment in the function of tight junctions between epithelial cells of the intestinal barrier gives rise to increased intestinal permeability and evaluation of intestinal mucositis, edema, and diarrhea (Wardill et al., 2012). This explanation resembles that which was reported previously in cases of brain edema (Bauer et al., 2010). MMP9, which is expressed mainly by neutrophils and macrophages (Mirastschijski et al., 2002), is incapable of digesting interstitial collagens and is upregulated in the healing of colon anastomoses (Seifert et al., 1996). Moreover, the overexpression of stromal MMP9 is related to decreased collagen deposition (Ågren et al., 1998), increased anastomotic leakage (Stumpf et al., 2005), and poor tissue repair (Watelet et al., 2005)

In the present results, ileum tissues showed different responses to glyphosate in terms of rat gender. The ileums of the female rats were more affected than that of males. These results are in agreement with those of Mesnage et al. (2017), who stated that female rats were more susceptible than male rats to toxins in Roundup herbicide. The findings are also consistent with the results reported by Turkmen & Dogan (2020), who demonstrated that female rats were more sensitive to glyphosate isopropylamine salt than male rats were. It can be suggested that this difference might have occurred because of the effect of some pesticides, which may intervene with the functional hormone of the female, leading to negative effects on the reproductive system and other organs.

In contrast, in the study by Barkai et al. (2019), female rats showed greater resistance than male rats, as females demonstrated better preservation of their hemodynamic and metabolic parameters during abdominal compartment syndrome than males did.

The exact reason for the difference in the responses to glyphosate in terms of rat gender is still not clear and requires further investigation.

Interestingly, there are numerous routes for humans to be exposed to glyphosate including food and drinking water which are both in occupational and environmental settings (Gillezeau et al., 2019). Furthermore, wind and water erosion are considered tools for the spread of glyphosate and its metabolites (Silva et al., 2018). Since glyphosate is used as an agricultural pesticide to control weeds, it has the potential to contaminate harvested food consumed by both humans and cattle (Bai & Ogbourne, 2016; Zhao et al., 2018). Thus, in our normal real life, because we consume foods like vegetables and fruits we may be exposed to glyphosate-Roundup on the daily basis. Importantly, the amount of ingested glyphosate is variable; depending on the amount used by farmers, the amount of contaminated food consumed, and also, how we wash and treat the food prior to consumption.

## Conclusion

To sum up, glyphosate-based herbicide results in considerable damage to the ileum structure of rats of both sexes. However, female rats were more affected than male rats were. Because of the anatomical, physiological, and genetic similarity of rats to humans, rats are considered the preferred species for biomedical research animal models. Thus, the present results could contribute basic information demonstrating the extent of the impact of glyphosate (Roundup) on public health and what care should be exercised during use of glyphosate herbicide in fields of growing plants and vegetables. Glyphosate should be applied in an accurate dose (according to the World Health Organization) to minimize its negative effects as much as possible. Alternatively, glyphosate should be replaced by normal herbicides such as organic herbicides, which can be obtained in the United States. Examples of organic herbicides include herbicidal soaps that use fatty acids to kill weeds and industrial vinegar containing larger amounts of acetic acid than what is normally available in kitchens. However, further biochemical and biological investigation must be carried out to get better understand of the toxicological impact of glyphosate on mammalians.

## Availability of data and materials

The data that support the findings of this study are available from the corresponding author upon reasonable request. https://orcid.org/0000-0001-7646-2592.

**Acknowledgment.** The authors acknowledge the Support of the Zoology and Entomology Department, Assiut University, Egypt.

**Authors contribution statement.** S.M.M.S. designed the experiment, practical work, practical analysis, and wrote the manuscript. T.A.E. contributed to the practical work. M.M.A. contributed in analyzing the results, discussing them, and participated in preparing the research and M.A.I.A. contributed his idea of work and review the manuscript.

**Conflict of interest.** The authors declare no potential conflict of interest.

## References

**Ågren MS, Jorgensen LN, Andersen M, Viljanto J & Gottrup F** (1998). Matrix metalloproteinase 9 level predicts optimal collagen deposition during early wound repair in humans. *Br J Surg* **85**, 68–71. doi:10.1046/j.1365-2168.1998.00556.x

**Bai SH & Ogbourne SM** (2016). Glyphosate: Environmental contamination, toxicity and potential risks to human health via food contamination. *Environ Sci Pollut Res* **23**, 18988–19001. doi:10.1007/s11356-016-7425-3

**Barkai O, Assalia A, Gleizarov E & Ahmad Mahajna A** (2019). Gender differences in response to abdominal compartment syndrome in rats. *BMC Res Notes* **12**, 321. doi:10.1186/s13104-019-4353-6

**Bauer AT, Bürgers HF, Rabie T & Marti HH** (2010). Matrix metalloproteinase-9 mediates hypoxia-induced vascular leakage in the brain via tight junction rearrangement. *J Cereb Blood Flow Metab* **30**, 837–848. doi:10.1038/jcbfm.2009.248

**Benbrook CM** (2016). Trends in glyphosate herbicide use in the United States and globally. *Environ Sci Eur* **28**(3), 1–15. doi:10.1186/s12302-016-0070-0

**Cathcart J, Pulkoski-Gross A & Cao J** (2015). Targeting matrix metalloproteinases in cancer: Bringing new life to old ideas. *Genes Dis* **2**, 26–34. doi:10.1016/j.gendis.2014.12.002

**Cheville NF** (1988). *Introduction to Veterinary Pathology*. Ames, IA: Iowa State University Press, 537 pp. Available at https://lib.ugent.be/catalog/rug01:000195559.

**Collado MC, Grześkowiak L & Salminen S** (2007). Probiotic strains and their combination inhibit in vitro adhesion of pathogens to pig intestinal mucosa. *Curr Microbiol* **55**(3), 260–265. doi:10.1007/s00284-007-0144-8

**Connolly A, Leahy M, Jones K, Kenny L & Coggins MA** (2018). Glyphosate in Irish adults—A pilot study in 2017. *Environ Res* **165**, 235–236. doi:10.1016/j.envres.2018.04.025

**Conrad A, Schröter-Kermani C, Hoppe W, Rüther M, Pieper S & Kolossa-Gehring M** (2016). Glyphosate in German adults – Time trend (2001 to 2015) of human exposure to a widely used herbicide. *J Hyg Environ Health* **220**, 8–16. doi:10.1016/j.ijheh.2016.09.016

**Drury RA & Wallington EA** (1980). *Carleton's Histological Techniques*, 5th ed. New York: Oxford University Press, p. 195.

**Duke SO** (1988). Glyphosate. In *Herbicides: Chemistry, Degradation, and Mode of Action*, Kearney PC & Kaufman DD (Eds.), pp. 1–70. New York: Dekker.

**Duncan M & Grant G** (2003). Oral and intestinal mucositis—Causes and possible treatments. *Aliment Pharmacol Ther* **18**, 853–874. doi:10.1046/j.1365-2036.2003.01784.x

**Elghareeb TA, Ahmed MAI, Mohamed IA, Ahmed SMM & Ezz El-Din HA** (2018). Synergistic action of glyphosate on novel pesticides against *Culex pipiens* L. (Diptera: Culicidae) mosquitoes under laboratory conditions. *Aust J Basic Appl Sci* **12**, 45–52. doi:10.22587/ajbas.2018.12.4.9

**El-Shenawy NS** (2009). Oxidative stress responses of rats exposed to Roundup and its active ingredient glyphosate. *Environ Toxicol Pharmacol* **28**(3), 379–385. doi:10.1016/j.etap.2009.06.001

**Fathi MA, Han G, Kang R, Shen D, Shen J & Li C** (2020). Disruption of cytochrome P450 enzymes in the liver and small intestine in chicken embryos in ovo exposed to glyphosate. *Environ Sci Pollut Res* **27**, 16865–16875. doi:10.1007/s11356-020-08269-3

**Gillezeau C, van Gerwen M, Shaffer RM, Rana I, Zhang L, Sheppard L & Taioli E** (2019). The evidence of human exposure to glyphosate: A review. *Environ Health* **18**, 1–14. doi:10.1186/s12940-018-0435-5

**Gomes MP, Smedbol E, Chalifour A, Hénaultethier L, Labrecque M, Lepage L, Lucotte M & Ph J** (2014). Alteration of plant physiology by glyphosate and its by-product aminomethylphosphonic acid: An overview. *J Exp Bot* **65**, 4691–4703. doi:10.1093/jxb/eru269

**Hamdamin PS, Rasul KH & Aziz FM** (2017). Histopathological effects of methomyl pesticide and mobile phone electromagnetic radiation on duodenum of male albino rats. *ZANCO J Pure Appl Sci* **29**(4), 1–11. doi:10.21271/ZJPAS.29.4.1

**Hasnain SZ, Wang H, Ghia JE, Haq N, Deng Y, Velcich A, Grencis R, David J, Thornton DJ & Khan WI** (2010). Mucin gene deficiency in mice impairs host resistance to an enteric parasitic infection. *Gastroenterology* **138**, 1763–1771. doi:10.1053/j.gastro.2010.01.045

**Hershko C & Patz J** (2008). Ironing out the mechanism of anemia in celiac disease. *Haematologica* **93**(12), 1761–1765. doi:10.3324/haematol.2008.000828

**Holm G, Norrgren L, Andresson T & Thuren A** (1993). Effects of exposure to food contaminated with PBDE, PCN or PCB on reproduction, liver morphology and cytochrome P450 activity in the three-spined stickleback, *Gasterosteus aculeatus*. *Aquatic Toxicol* **27**, 33–50. doi:10.1016/0166-445X(93)90045-3

**Kiernan JA** (2001). *Histological and Histochemical Methods: Theory and Practice*, 3rd ed. London, New York and New Delhi: Arnold Publisher, pp. 111–162 and 219–240. doi:10.1016/j.ijheh.2016.09.016

**Kosik-Bogacka DI & Kolasa A** (2012). Histopathological changes in small and large intestines during hymenolepidosis in rats. *Folia Biol* **60**(3–4), 195–198. doi:10.3409/fb60_3-4.195-198

**Lazăr L, Loghin A, Bud ES, Cerghizan D, Horváth E & Nagy EE** (2015). Cyclooxygenase-2 and matrix metalloproteinase-9 expressions correlate with tissue inflammation degree in periodontal disease. *Rom J Morphol Embryol* **56**(4), 1441–1446.

**Ma T, Iwamoto GK, Hoa NT, Akotia V, Pedram A, Boivin MA & Said HM** (2004). TNF-alpha-induced increase in intestinal epithelial tight junction permeability requires NF-kappa B activation. *Am J Physiol Gastrointest Liver Physiol* **286**, G367–G376. doi:10.1152/ajpgi.00173.2003

**Mesnage R, Defarge N, de Vendômois JS & Séralini GE** (2015). Potential toxic effects of glyphosate and its commercial formulations below regulatory limits. *Food Chem Toxicol* **84**, 133–153. doi:10.1016/j.fct.2015.08.012

**Mesnage R, Renney G, Séralini GF, Ward M & Antoniou M** (2017). Multiomics reveal non-alcoholic fatty liver disease in rats following chronic exposure to an ultra-low dose of Roundup herbicide. *Sci Rep* **6**, 1–15. doi:10.1038/srep39328

**Mirastschijski U, Impola U, Jahkola T, Karlsmark T, Ågren MS & Saarialho-Kere U** (2002). Ectopic localization of matrix metalloproteinase-9 in chronic cutaneous wounds. *Hum Pathol* **33**, 355–364. doi:10.1053/hupa.2002.32221

**Mohamed IA, Ahmed MAI & Saba RM** (2016). Unique efficacy of certain novel herbicides against *Culex pipiens* (Diptera: Culicidae) larvae mosquito under laboratory conditions. *Adv Environ Biol* **10**, 104–111.

**Olaleye SB, Adaramoye OA, Erigbali PP & Adeniyi OS** (2007). Lead exposure increases oxidative stress in the gastric mucosa of HCl/ethanol-exposed rats. *World J Gastroenterol* **13**, 5121. doi:10.3748/wjg.v13.i38.5121

**Olubuyide IO, Williamson RC, Bristol JB & Read AE** (1984). Goblet cell hyperplasia is a feature of the adaptive response to jejunoileal bypass in rats. *Gut* **25**(1), 62–68. doi:10.1136/gut.25.1.62

**O'Sullivan S, Gilmer JF & Medina C** (2015). Matrix metalloproteinases in inflammatory bowel disease: An update. *Mediators Inflamm*, 1–15. doi:10.1155/2015/964131

**Pérez GL, Vera MS & Miranda L** (2011). Effects of herbicide glyphosate and glyphosate-based formulations on aquatic ecosystems. In *Herbicides and Environment*, Kortekamp A (Ed.). Rijeka, Croatia: In Tech Publications. ISBN:978-953-307-476-4. doi:10.5772/12877.

**Ramírez-Duarte WF, Iang S, Rondón-Barragán IS & Eslava-Mocha PR** (2008). Acute toxicity and histopathological alterations of Roundup® herbicide on "cachama blanca" (*Piaractus brachypomus*). *Pesqui Vet Bras* **28**(11), 547–554.

**Ruppel ML, Brightwell BB, Schaefer J & Marvel JT** (1977). Metabolism and degradation of glyphosate in soil and water. *J Agric Food Chem* **25**, 517–528. doi:10.1021/jf60211a018

**Saba RM, Mohamed IA & Ahmed MAI** (2018). Toxicological and biochemical investigation of certain herbicides on *Culex pipiens* L. (Diptera: Culicidae) mosquitos under laboratory conditions. *Adv Nat Appl Sci* **12**, 6–12. doi:10.22587/anas.2018.12.2.2

**Saleh SHMM, Elghareeb TA, Ahmed MAI, Mohamed IA & El-Din HAE** (2018). Hepato-morpholoy and biochemical studies on the liver of albino rats after exposure to glyphosate-Roundup®. *J Basic Appl Zool* **79**, 48. doi:10.1186/s41936-018-0060-4

**Samanta P, Pal S, Mukherjee AK & Ghosh AR** (2016*b*). Pathological (histological and ultrastructural) study in stomach and intestine of *Heteropneustes fossilis* (Bloch) to excel Mera 71, a glyphosate-based herbicide. *J Gastrointest Dig Syst* **6**, 6. doi:10.4172/2161-069X.1000479

**Samanta P, Pal S, Mukherjee AK, Senapati T & Ghosh AR** (2016*a*). Histopathological and ultrastructural alterations in *Anabas testudineus* exposed to glyphosate-based herbicide, Excel Mera 71 under field and laboratory conditions. *J Aquac Res Dev* **7**, 436. doi:10.4172/2155-9546.1000436

**Samsel A & Seneff S** (2013). Glyphosate's suppression of cytochrome P450 enzymes and amino acid biosynthesis by the gut microbiome: Pathways to modern diseases. *Entropy* **15**, 1416–1463. doi:10.3390/e15041416

**Seifert WF, Wobbes T & Hendriks T** (1996). Divergent patterns of matrix metalloproteinase activity during wound healing in ileum and colon of rats. *Gut* **39**, 114–119. doi:10.1136/gut.39.1.114

**Senapati T, Mukrjee AK & Ghosh AR** (2009). Observations on the effect of glyphosate based herbicide on ultra structure (SEM) and enzymatic activity in different regions of alimentary canal and gill of *Channa punctatus* (Bloch). *J Crop Weed* **5**(1), 233–242.

**Silva V, Montanarella L, Jones A, Fernandez-Ugalde O, Mol HGJ, Ritsema CJ & Geissen V** (2018). Distribution of glyphosate and aminomethylphosphonic acid (AMPA) in agricultural topsoils of the European Union. *Sci Total Environ* **621**, 1352–1359. doi:10.1016/j.scitotenv.2017.10.093

**Stumpf M, Klinge U, Wilms A, Zabrocki R, Rosch R, Junge K, Krones C & Schumpelick V** (2005). Changes of the extracellular matrix as a risk factor for anastomotic leakage after large bowel surgery. *Surgery* **137**, 229–234. doi:10.1016/j.surg.2004.07.011

**Tooley KL, Howarth GS & Butler RN** (2009). Mucositis and non-invasive markers of small intestinal function. *Cancer Biol Ther* **8**, 753–758. doi:10.4161/cbt.8.9.8232

**Torretta V, Katsoyiannis I, Viotti P & Rada E** (2018). Critical review of the effects of glyphosate exposure to the environment and humans through the food supply chain. *Sustainability* **10**(4), 95. doi:10.3390/su10040950

**Turkmen R, Birdane YO, Demirel HH, Yavuz H, Kabu M & Ince S** (2019). Antioxidant and cytoprotective effects of N-acetylcysteine against subchronic oral glyphosate-based herbicide-induced oxidative stress in rats. *Environ Sci Pollut Res* **26**, 11427–11437. doi:10.1007/s11356-019-04585-5

**Turkmen R & Dogan I** (2020). Determination of acute oral toxicity of glyphosate isopropylamine salt in rats. *Environ Sci Pollut Res* **27**, 19298–19303.

**Vandooren J, Van den Steen PE & Opdenakker G** (2013). Biochemistry and molecular biology of gelatinase B or matrix metalloproteinase-9 (MMP9): The next decade. *Crit Rev Biochem Mol Biol* **48**, 222–272. doi:10.3109/10409238.2013.770819

**Walter JB & Isreal MS** (1974). *General Pathology*, 4th ed. Edinburgh, London, New York: Churchill Livingstone, p. 681. doi:10.1002/path.1711580117

**Wardill HR, Bowen JM & Gibson RJ** (2012). Chemotherapy-induced gut toxicity: Are alterations to intestinal tight junctions pivotal? *Cancer Chemother Pharmacol* **70**, 627–635. doi:10.1007/s00280-012-1989-5

**Watelet JB, Demetter P, Claeys C, Van Cauwenberge P, Cuvelier C & Bachert C** (2005). Neutrophil-derived metalloproteinase-9 predicts healing quality after sinus surgery. *Laryngoscope* **115**, 56–61. doi:10.1097/01.mlg.0000150674.30237.3f

**Woods AE & Stirling JW** (2008). Electron microscopy. In *Theory and Practice of Histological Techniques*, 6th ed., Bancroft JD & Gamble M (Eds.), pp. 601–636. Edinburgh: Churchill Livingstone Elsevier.

**Zhao J, Pacenka S, Wu J, Brian K, Richards BK, Steenhuis T, Simpson K & Hay AG** (2018). Detection of glyphosate residues in companion animal feeds. *Environ Pollut* **243**, 1113–1118. doi:10.1016/j.envpol.2018.08.100